

Progresses on 148 nm light sources for precision measurement of nuclear transition of ^{229m}Th

Yang Wang(王样), Zheng-Rong Xiao(肖峥嵘), Heng-Zhi Zhang(张恒之), Lin-Qiang Hua(华林强), and Xiao-Jun Liu(柳晓军)

Citation: Chin. Phys. B, 2026, 35 (**2**): 020601. DOI: 10.1088/1674-1056/ae0d78

http://cpb.iphy.ac.cn; http://iopscience.iop.org/cpb

What follows is a list of articles you may be interested in

Progresses on Th-doped materials for solid-state nuclear clock

Cheng-Chun Zhao(赵呈春), Lin Li(李琳), Shan-Ming Li(李善明), Qiao-Rui Gong(龚巧瑞), Pei-Xiong Zhang(张沛雄), Yin Hang(杭寅), Long-Sheng Ma(马龙生), and Shi-Ning Zhu(祝世宁)

Chin. Phys. B, 2026, 35 (**2**): 020602. DOI: 10.1088/1674-1056/ae210f

A Yb optical clock with a lattice power enhancement cavity

Chunyun Wang(王春云), Yuan Yao(姚远), Haosen Shi(师浩森), Hongfu Yu(于洪浮),Longsheng Ma(马龙生), and Yanyi Jiang(蒋燕义)

Chin. Phys. B, 2024, 33 (**3**): 030601. DOI: 10.1088/1674-1056/ad1986

Sympathetic electromagnetically induced transparency ground state cooling of a $^{40}Ca^{+}$–$^{27}Al^{+}$ pair in an $^{27}Al^{+}$ clock

Chenglong Sun(孙成龙), Kaifeng Cui(崔凯枫), Sijia Chao(晁思嘉), Yuanfei Wei(魏远飞), Jinbo Yuan(袁金波), Jian Cao(曹健), Hualin Shu(舒华林), and Xueren Huang(黄学人)

Chin. Phys. B, 2023, 32 (**5**): 050601. DOI: 10.1088/1674-1056/aca39d

Laboratory demonstration of geopotential measurement using transportable optical clocks

Dao-Xin Liu(刘道信), Jian Cao(曹健), Jin-Bo Yuan(袁金波), Kai-Feng Cui(崔凯枫), Yi Yuan(袁易),Ping Zhang(张平), Si-Jia Chao(晁思嘉), Hua-Lin Shu(舒华林), and Xue-Ren Huang(黄学人)

Chin. Phys. B, 2023, 32 (**1**): 010601. DOI: 10.1088/1674-1056/ac6337

Study of optical clocks based on ultracold ^{171}Yb atoms

Di Ai(艾迪), Hao Qiao(谯皓), Shuang Zhang(张爽), Li-Meng Luo(骆莉梦), Chang-Yue Sun(孙常越), Sheng Zhang(张胜), Cheng-Quan Peng(彭成权), Qi-Chao Qi(齐启超), Tao-Yun Jin(金涛韫), Min Zhou(周敏), Xin-Ye Xu(徐信业)

Chin. Phys. B, 2020, 29 (**9**): 090601. DOI: 10.1088/1674-1056/aba099

TOPICAL REVIEW — Advances in thorium nuclear optical clocks

Progresses on 148 nm light sources for precision measurement of nuclear transition of ^{229m}Th

Yang Wang(王样)[1,2,†], Zheng-Rong Xiao(肖峥嵘)[1,2,†], Heng-Zhi Zhang(张恒之)[1,2], Lin-Qiang Hua(华林强)[1,2,‡], and Xiao-Jun Liu(柳晓军)[1,2,§]

[1] *State Key Laboratory of Magnetic Resonance and Atomic and Molecular Physics, Wuhan Institute of Physics and Mathematics, Innovation Academy for Precision Measurement Science and Technology, Chinese Academy of Sciences, Wuhan* 430071, *China*

[2] *School of Physical Sciences, University of Chinese Academy of Sciences, Beijing* 100049, *China*

(Received 31 July 2025; revised manuscript received 25 September 2025; accepted manuscript online 30 September 2025)

The thorium-229 nucleus possesses a uniquely low-energy nuclear transition (~ 8.4 eV, corresponding to a wavelength of ~ 148 nm), which is the first confirmed nuclear excitation that can be coherently manipulated by narrow-linewidth lasers. Consequently, this transition has garnered widespread interest over the past decades. Owing to the small nuclear size and strong resistance to environmental perturbations, a thorium-based nuclear clock is theoretically capable of achieving an unprecedented fractional frequency uncertainty at the 10^{-20} level, offering great promise as a next-generation frequency standard. Among the key ingredients of such a thorium-based nuclear clock, a high-performance 148 nm excitation source is of critical importance. Since the feasibility of directly exciting the transition, as well as the overall clock performance, depends heavily on the availability and quality of such a source, the development of high-quality 148 nm laser sources represents a frontier for scientists worldwide. In this article, we provide a systematic overview of the current development of 148 nm laser sources. First, we briefly introduce the scientific motivation for high-precision spectroscopy of the thorium nuclear transition and the corresponding technical requirements for 148 nm laser sources. Then, we summarize four main types of existing 148 nm source generation schemes and their working principles, along with recent progress in nuclear transition measurements using such sources. Finally, we discuss potential future directions.

Keywords: thorium-229, 148 nm laser, optical clock, four-wave mixing, VUV combs

PACS: 06.30.Ft, 42.65.Ky, 42.72.Ai

DOI: 10.1088/1674-1056/ae0d78 **CSTR:** 32038.14.CPB.ae0d78

1. Introduction

Among the more than 3000 known nuclides, thorium-229 has a nuclear transition that is lower in energy (only 8.4 eV) than almost every other known nuclear transition, and has therefore received considerable attention.[1] This excited state, referred to as ^{229m}Th, is a metastable isomeric state of the thorium-229 nucleus. Its transition wavelength is approximately 148 nm, which lies within the vacuum ultraviolet (VUV) region, accessible by modern laser technology. This unique feature enables precise control of nuclear states using laser-based techniques. Compared to electronic transitions, this nuclear transition offers several significant advantages. First, the spatial scale of the nucleus is about three orders of magnitude smaller than that of the atom, making it less susceptible to spatial inhomogeneities of electromagnetic fields under similar conditions. Second, the electrons surrounding the nucleus provide natural shielding, which significantly reduces the sensitivity of the nucleus to external electromagnetic perturbations. Third, the excited nuclear state exhibits an extremely narrow linewidth and an exceptionally long lifetime (exceeding 1000 seconds), resulting in a quality factor (Q) on the order of 10^{19}.[2–7] Thus, optical clock systems based on the ^{229}Th nuclear transition can achieve superior frequency stability. Theoretically, the stability of a nuclear clock based on this transition could reach the 10^{-19} level,[8] making it a promising candidate for the next generation of time and frequency standards.

The low transition energy arises from a near cancellation between the change in Coulomb energy between the isomers, which depends linearly on the dimensionless fine-structure constant α, and the contribution from the nuclear force, which exhibits only weak α dependence. This cancellation leads to an extremely low transition energy ($E = 8.4$ eV) compared to typical nuclear transitions. Consequently, any change in α or the Coulomb energy leads to a relative change several orders of magnitude larger in the transition energy. According to theoretical calculations, the enhancement factor for α variation is $K = -(0.82 \pm 0.25) \times 10^4$, which is much higher than the typical values of $K \sim 0.1$–6 for current atomic clocks.[9–15] This characteristic makes the ^{229}Th nuclear transition an ideal

†These authors contributed equally to this work.
‡Corresponding author. E-mail: hualq@wipm.ac.cn
§Corresponding author. E-mail: xjliu@wipm.ac.cn

© 2026 Chinese Physical Society and IOP Publishing Ltd. All rights, including for text and data mining, AI training, and similar technologies, are reserved.

platform for testing temporal variation of α, exploring fundamental questions such as dark matter, testing physics beyond the Standard Model, and investigating the Einstein equivalence principle. Thus, the thorium nuclear clock holds great promise not only for timekeeping but also for fundamental physics research.[16]

Owing to its significance, the nuclear transition in ^{229m}Th has been a focal point of global research for nearly 50 years. In 1976, Kroger and Reich[17] measured the γ spectrum of ^{229}Th produced by the α-decay of ^{233}U, and their analysis provided the first indication of the ^{229m}Th nuclear isomeric transition. Over the following decades, researchers have employed a range of advanced techniques — including high-resolution detectors, magnetic microcalorimeters, and precise γ-ray energy and branching ratio measurements — to improve the accuracy of nuclear transition energy determinations. These efforts have ultimately constrained the transition energy to approximately 8.4 eV.[18–20] In 2024, researchers from the Physikalisch-Technische Bundesanstalt (PTB)[21] and the University of California, Los Angeles (UCLA)[7] successfully achieved laser excitation of the ^{229}Th nuclear transition using GHz-linewidth four-wave-mixing pulsed light sources. These experiments employed ^{229}Th-doped CaF_2 and $LiSrAlF_6$ crystals, respectively, and the transition wavelength was precisely determined to be 148.382 nm. Subsequently, by using a vacuum ultraviolet (VUV) frequency comb, the Joint Institute for Laboratory Astrophysics (JILA) research team established a direct frequency link between the ^{229m}Th isomeric transition and the ^{87}Sr atomic clock, determined the absolute transition frequency to the kHz level, and directly resolved the narrow line structure arising from the interaction between the nuclear electric quadrupole moment and the crystal electric field gradient.[2] With these breakthroughs, the development of the thorium nuclear optical clock entered a phase of rapid progress.

These research developments demonstrated that breakthroughs in thorium nuclear transition measurements require both precise manipulation of thorium systems and high-quality 148 nm radiation sources. The natural linewidth of this nuclear transition is only 80 ± 20 μHz.[3] This necessitates that the excitation light source not only possess an ultra-narrow linewidth to match the extremely narrow bandwidth of the nuclear transition, but also exhibit sufficiently high power density to overcome the inherently low transition probability and the resulting limitations in excitation efficiency. Moreover, the thorium nuclear transition at 148 nm lies within the VUV spectral range, which is well beyond the operational limits of conventional nonlinear crystals. Most crystalline materials either exhibit strong absorption or encounter severe phase-matching challenges in this spectral region, rendering conventional nonlinear frequency conversion approaches ineffective. Consequently, the realization of practical laser sources at this wavelength necessitates either gas-phase nonlinear conversion schemes or the development of specialized nonlinear crystals with VUV transparency.

Through persistent efforts, scientists have successfully developed several types of 148 nm light sources capable of exciting the thorium nuclear transition. These currently available sources include synchrotron radiation, gas-phase four-wave-mixing pulsed sources, high-harmonic-generation-based VUV frequency combs, and 148 nm continuous-wave lasers. In the following sections, we provide a detailed introduction to these critical light sources.

2. Synchrotron radiation-based 148 nm light sources

Synchrotron radiation is electromagnetic radiation emitted when relativistic charged particles undergo acceleration perpendicular to their velocity. This phenomenon was first observed around 1947.[22] When electrons circulate in a storage ring at near-light speeds, the Lorentz force induced by bending magnets causes them to emit highly intense and highly collimated electromagnetic radiation.[23]

A synchrotron radiation facility typically consists of six main components: an electron injector, an electron transport line, a storage ring, insertion devices, beamline systems, and experimental stations. A representative example is the Super Photon Ring-8 (SPring-8, as shown in Fig. 1) facility, a third-generation large-scale synchrotron radiation facility jointly operated by the Rikagaku Kenkyūjo (RIKEN) and the Japan Synchrotron Radiation Research Institute (JASRI) in Japan.[24] The electrons emitted by the electron gun are accelerated to 8 GeV by the accelerator, injected into a storage ring with a circumference of about 1500 m, and circulated while maintaining an energy of 8 GeV. To further enhance the brightness and spectral tunability of the emitted radiation, the storage ring is equipped with a variety of insertion devices, including standard undulators, elliptical wigglers, and double-helical undulators. These devices enable the generation of highly coherent radiation spanning from the VUV to the hard x-ray region. The generated synchrotron radiation is guided through the beamline to experimental stations located inside and outside the storage ring building and is used for a wide range of experiments.

At a time when the energy of the ^{229}Th nuclear transition was still uncertain on the order of eV, early experimental efforts focused on using high-brightness synchrotron radiation sources to induce excitation. However, in most cases, direct observation of the transition to the isomeric state was not achieved. For example, in 2015, Jeet *et al.*[25] used the Advanced Light Source (ALS) synchrotron to expose ^{229}Th-doped $LiSrAlF_6$ crystals with 7.3–8.8 eV VUV photons and

did not observe any resulting fluorescence from ^{229m}Th. Although no evidence of the thorium nuclear transition was observed, this measurement excluded roughly half of the favored transition search range and provided valuable guidance for subsequent experiments. In 2018, Stellmer *et al.*[26] performed a similar direct excitation experiment using the ALS synchrotron, and no signatures of the nuclear transition were detected. These results suggested that the transition may possess an exceptionally narrow bandwidth or that its energy may differ significantly from earlier expectations.

In 2019, Masuda *et al.*[27] used narrow-band 29 keV synchrotron radiation from SPring-8 to resonantly excite the second excited nuclear state, which predominantly (about 58%) decays into the isomer, thereby effectively generating the ^{229m}Th nuclear isomer state through an indirect process. Their study not only precisely determined the energy of the second excited state (29189.93 ± 0.07 eV) and its half-life (82.2 ± 4.0 ps), but also further constrained the possible energy range of the isomeric state to 2.5–8.9 eV. This work motivated the community to pursue direct laser excitation of the first excited state. In 2024, Yamaguchi *et al.*[5] also used narrow-band 29 keV synchrotron radiation from SPring-8 to excite the nuclear transition in a VUV-transparent ^{229}Th-doped CaF_2 crystal. The transition wavelength of the metastable state was determined to be $148.18 \pm 0.38_{(\mathrm{stat})} \pm 0.19_{(\mathrm{syst})}$ nm.

Although precise optical clock operation based on the thorium nuclear transition has not yet been realized, synchrotron radiation facilities in China are capable of delivering high-quality 148 nm or 29.2 keV light sources for such investigations. For example, the second-generation Beijing Synchrotron Radiation Facility (BSRF) can provide UV–VUV light covering a wavelength range from 360 nm to 120 nm.[28] The third-generation Shanghai Synchrotron Radiation Facility (SSRF) operates a VUV beamline with first-order radiation covering the photon energy range 7–165 eV.[29]

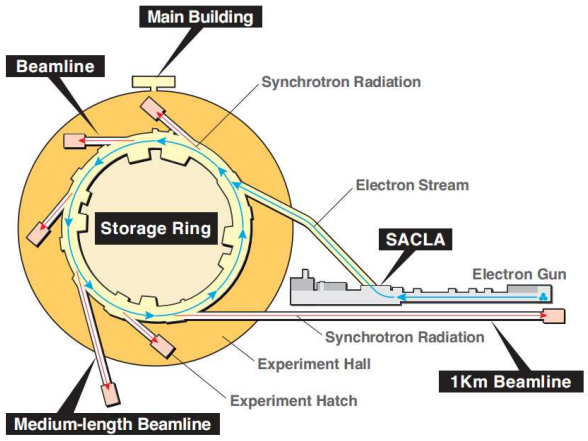


Fig. 1. Schematic diagram of the SPring-8 synchrotron radiation facility.[24]

3. Four-wave mixing-based 148 nm pulsed light source

To achieve enhanced spectral selectivity and higher excitation efficiency, researchers have turned to light sources based on resonance-enhanced four-wave mixing (FWM) processes in gaseous media. Using this advanced light source, researchers have for the first time achieved direct laser excitation of the first excited state of ^{229}Th. This milestone represents a substantive breakthrough in thorium nuclear excitation research. In the following section, we introduce the principle of the FWM process and present experimental work on ^{229}Th nuclear transition excitation and measurement using FWM-based 148 nm pulsed light sources.

When a strong laser propagates through a nonlinear medium, it induces polarization in the medium, with the polarization strength depending on the electric field of the laser. This relationship can be expressed as

$$P = \varepsilon_0\left(\chi^{(1)}E(\omega) + \chi^{(2)}E(\omega_1)E(\omega_2) + \chi^{(3)}E(\omega_1)E(\omega_2)E(\omega_3) + \cdots\right). \tag{1}$$

In the above expression, P denotes the polarization strength, ε_0 is the vacuum permittivity, $\chi^{(1)}$ is the linear susceptibility, and $\chi^{(n)}$ denotes the n^{th}-order nonlinear susceptibility. FWM is a third-order nonlinear optical process in which three driving laser beams — with wave vectors $\tilde{k}_1$, $\tilde{k}_2$, $\tilde{k}_3$ and corresponding frequencies ω_1, ω_2, ω_3 — interact with a nonlinear medium to generate a fourth beam with wave vector $\tilde{k}_4$ and frequency ω_4, as illustrated in Fig. 2. The generation of four-wave mixing in the VUV region typically requires a nonlinear medium with a nonzero third-order nonlinear susceptibility $\chi^{(3)}$ (commonly inert gases) and must simultaneously satisfy the conditions of energy and momentum conservation, expressed as

$$\omega_1 + \omega_2 - \omega_3 = \omega_4, \tag{2}$$

$$\tilde{k}_1 + \tilde{k}_2 + \tilde{k}_3 + \tilde{k}_4 = 0. \tag{3}$$

As a typical FWM laser source demonstrated by Peik *et al.*[21] from PTB, the VUV laser source generation system consists of two continuous-wave (CW) Ti:sapphire (Ti:Sa) ring lasers with two pulsed dye amplification stages, a third-harmonic generation (THG) unit, and a Xe gas cell for four-wave mixing, as illustrated in Fig. 3. It operates at a repetition rate of 30 Hz, with a pulse duration of 10 ns and a mean pulse energy of ~ 15 μJ over the wavelength range 148.3–149.1 nm. The VUV source provides a spectral photon flux exceeding 2×10^4 photons/(s·Hz),[30] with a spectral linewidth of ≤ 10 GHz. This corresponds to a VUV power spectral density of ~ 0.1 pW/Hz.

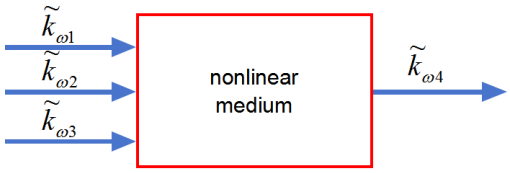


Fig. 2. Schematic diagram of the four-wave mixing.

Using this laser system, the Peik research group carried out VUV excitation experiments on trapped Th^+ ions in 2023. The system was designed to operate over a wide scanning range from 148 nm to 155 nm. The source produces pulses with durations of 6–10 ns and energies of up to 40 μJ, and is coupled via a vacuum beamline to a linear radiofrequency ion trap. In the first implementation of VUV laser spectroscopy of trapped Th^+ ions, three previously unknown resonance lines near 148 nm were excited, with the upper states lying close to the Th-229 isomer state. The resonances were detected and analyzed via fluorescence from the excited Th^+ ions. After subtracting a Doppler broadening of 2.7 GHz, the linewidth of the VUV radiation was estimated to be ≤ 6 GHz, mainly limited by phase noise amplified during the harmonic generation and four-wave mixing processes. This result confirms that the pulsed FWM light source possesses high spectral resolution and tunability, fulfilling the requirements for nuclear spectroscopy excitation.[30]

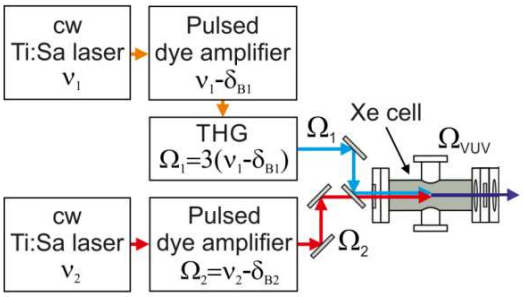


Fig. 3. Experimental setup[21] of the FWM laser source at PTB, Germany.

Subsequently, in 2024, the same research group used the VUV laser to excite ^{229}Th-doped CaF_2 crystals. Under cryogenic conditions (< 180 K) and high vacuum (10^{-5} Pa) to minimize background signals and suppress non-radiative processes, a resonance fluorescence signal was observed in two crystals with different Th-229 dopant concentrations, while it was absent in a comparison experiment using Th-232, marking the first realization of direct laser excitation of the ^{229}Th nucleus to the first excited state. The nuclear resonance for Th^{4+} ions in Th:CaF_2 was measured to be 2020.409(7) THz, and the fluorescence lifetime in the crystal was 630(15) s, corresponding to an isomer half-life of 1740(50) s for a nucleus isolated in vacuum or a transition rate of $B(M1) = 0.022$ in Weisskopf units (W.u.).[21]

Almost simultaneously, the Hudson group from UCLA also realized direct laser excitation of the ^{229}Th nucleus to the first excited state using a pulsed FWM VUV laser source. The crystal employed in this work was ^{229}Th:$LiSrAlF_6$, and the transition frequency was determined to be $2020407.3(5)_{stat}(30)_{sys}$ GHz ($148.38219(4)_{stat}(20)_{sys}$ nm), with a measured lifetime of $568(13)_{stat}(20)_{sys}$ s. This study confirms the feasibility of exciting the ^{229}Th nuclear transition in doped crystals.[7]

In the same year, a collaboration between the Ye group from JILA and the Hudson group from UCLA realized direct laser excitation of the ^{229}Th nucleus in thin-film $^{229}ThF_4$ targets using a pulsed FWM VUV laser source. Thin-film $^{229}ThF_4$ targets with thicknesses of 30–100 nm were fabricated by miniaturized radioactive physical vapor deposition (PVD) on different substrates, including Al_2O_3 and MgF_2. A single peak was observed at $2020406.8(4)_{stat}(30)_{sys}$ GHz for the $^{229}ThF_4$ film on the MgF_2 substrate and at $2020409.1(7)_{stat}(30)_{sys}$ GHz on the Al_2O_3 substrate. This work laid the foundation for the future development of simple and portable solid-state nuclear clocks.[31]

In contrast to previous studies using thin-film $^{229}ThF_4$ targets, the Hudson group[32] from UCLA very recently reported measurements performed using a thin $^{229}ThO_2$ target. In this work, a laser-based conversion-electron detection scheme was realized for the first time, paving the way toward nuclear clocks based on conversion electrons. The transition frequency was measured to be $2020407.5(2)_{stat}(30)_{sys}$ GHz, and the internal conversion decay channel was found to have a lifetime of approximately 10 μs. The excitation laser source was the same pulsed FWM VUV laser system.

In China, a research group led by Mo[33] at Tsinghua University has developed a wavelength-tunable VUV/extreme ultraviolet (XUV) laser source using a two-photon resonance-enhanced four-wave mixing technique in Kr/Xe gas. The resulting radiation covers an effective energy range of 8.0–14.0 eV. This setup is presently intended for applications in high-resolution spectroscopy and mass spectrometric imaging.

4. VUV frequency comb-based 148 nm light source

Following the realization of direct laser excitation, researchers introduced a VUV frequency comb system to further improve the precision of transition frequency measurements, achieving kHz-level accuracy for the first time.[2]

4.1. Basic configuration of the VUV frequency comb system

A frequency comb is a laser source whose spectrum consists of a series of equally spaced frequency components. This comb-like spectral structure arises from a train of femtosecond pulses emitted by a mode-locked laser, where periodic pulses in the time domain correspond to evenly spaced "teeth" in the

frequency domain. Owing to its excellent temporal coherence and frequency stability, the optical frequency comb has become an indispensable tool in modern precision measurement.

The pulse train emitted by a mode-locked laser appears in the time domain as a Dirac comb function

$$III_T(t) = \sum_{n=-\infty}^{\infty} \delta(t - nT). \tag{4}$$

The Fourier transform of the Dirac comb function is

$$III_T(t) \xrightarrow[F]{I} II_{\frac{1}{T}}(f). \tag{5}$$

Assuming that the pulse repetition rate of the mode-locked laser is stable and that the phase difference between successive pulses remains constant, the resulting femtosecond pulse train forms a comb-like structure in the frequency domain, as illustrated in Fig. 4. In practice, there is an offset between the first comb tooth and zero frequency, known as the carrier-envelope offset frequency. The frequency of each comb tooth, f_n, is given by $f_n = n \times f_r + f_0$, where f_r is the pulse repetition frequency and f_0 denotes the carrier-envelope offset frequency.

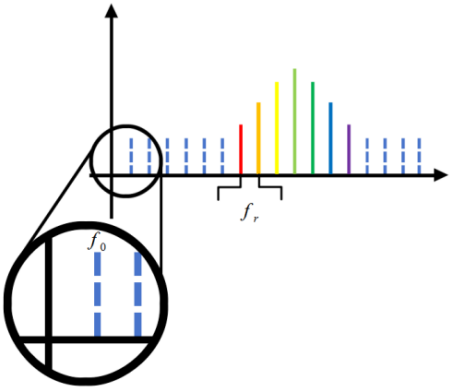


Fig. 4. Schematic diagram of the frequency comb.

Through nonlinear frequency conversion techniques such as sum-frequency generation (SFG) or harmonic generation, the spectral coverage of an optical frequency comb can span from the ultraviolet to the mid-infrared (MIR) range using nonlinear crystals. However, due to the lack of suitable nonlinear crystals in the VUV/XUV band, direct generation of frequency combs in this spectral region via conventional methods is unfeasible. Consequently, high-harmonic generation (HHG) in gaseous media has become the main viable approach for spectral extension into the VUV and XUV regimes.

Spectral extension into the VUV band via HHG faces a critical challenge, namely the achievement of sufficiently high peak intensities ($> 10^{13}$ W/cm^2)[34] to drive the nonlinear process efficiently. A femtosecond frequency comb laser typically operates at a relatively high repetition rate of around 100 MHz to maintain its excellent temporal coherence. To achieve the peak intensities required for HHG, the average laser power must reach the kW level. This necessitates the implementation of a femtosecond enhancement cavity (fsEC) for power scaling.

A fsEC is a type of Fabry–Pérot interferometer that can be designed to increase the intracavity power. When the length of the cavity matches the repetition period of the laser pulses, a stable coherently enhanced field is formed inside the cavity. Figure 5 shows the structure of a fsEC, which is composed of six mirrors. One of them serves as the input coupling mirror, allowing infrared femtosecond pulses to be injected into the cavity, while the remaining five are high-reflectivity mirrors that maintain stable circulation of the light within the cavity. Two concave mirrors are used to focus the laser into a small spot within the cavity, where the local intensity reaches the threshold required to drive high-order harmonic generation. Through mode matching and the application of the Pound–Drever–Hall (PDH) locking technique, femtosecond pulses can be stably resonated in the cavity, fulfilling the peak power requirement for efficient HHG. In the focal region of the enhancement cavity, an inert gas beam (such as xenon) is injected. Within the intensified laser field, the gas medium undergoes tunnel ionization; electrons are liberated and subsequently accelerated away from, and then driven back toward their parent ions by the oscillating laser field. A small fraction of these electrons recombine with the parent ion, emitting high-energy photons in this process. This cycle repeats periodically, generating multiple odd-order harmonics — this is known as the three-step model of HHG.[35] Due to the excellent coherence properties of HHG, each generated harmonic retains the frequency spacing and phase stability of the original infrared frequency comb. As a result, a VUV frequency comb is formed.

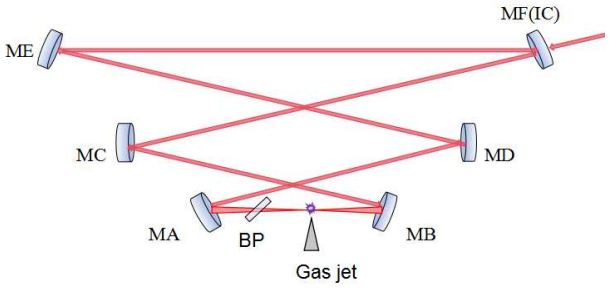


Fig. 5. Schematic diagram of the fsEC. MA–MF are high-reflectivity mirrors, with MA and MB being concave mirrors and MF (IC) serving as the input coupling mirror. BP denotes a Brewster plate, and the gas nozzle is placed at the focal point.

In 2005, the group of Ye[36] from JILA and the group of Hänsch[37] from Max–Planck–Institut für Quantenoptik (MPQ) independently reported the generation of coherent radiation in the VUV/XUV using HHG within a fsEC, marking the birth of the VUV/XUV optical frequency comb. In 2012, Cingöz *et al.*[38] performed direct frequency-comb spectroscopy using the 13$^{\text{th}}$ harmonic at 82 nm in argon atoms

($3s^23p^6 \rightarrow 3s^23p^55d$). The uncertainty of this transition was measured to be about 3 MHz, and the upper bound of the 13th-harmonic comb linewidth was determined to be less than 10 MHz, providing clear evidence that the XUV frequency comb exhibits a well-defined comb structure. In 2013, Pupeza *et al.*[39] coupled out the generated radiation through a pierced mirror. Harmonics up to an order of 91, corresponding to 11.45 nm or 108 eV, were obtained. This represents the shortest-wavelength XUV frequency comb demonstrated to date, approaching the soft x-ray region. In 2014, Benko *et al.*[40] performed a heterodyne beating measurement between harmonics generated by two separate XUV frequency comb systems driven by the same optical comb. They measured a beat-note linewidth of 62.5 mHz for the 17th harmonic, confirming that the XUV comb possesses a coherence time exceeding one second. In 2018, Porat *et al.*[41] used high-temperature gas mixtures as the generation medium to increase the gas translational velocity, thereby achieving phase-matched XUV frequency comb generation. They demonstrated an XUV comb output at 97 nm with a power of 2 mW, which remains the highest-power XUV frequency comb reported to date.

5. Measurement of the nuclear transition based on the 148 nm VUV frequency comb

Building on measurements with 148 nm pulsed lasers via four-wave mixing, researchers have started excitation of the ^{229}Th nuclear transition with VUV frequency combs. In 2024, the research group led by Ye[2] from JILA successfully realized the direct excitation of the ^{229}Th nuclear transition with a VUV optical frequency comb system. They stabilized the fundamental frequency comb to the JILA ^{87}Sr clock[42] and coherently up-converted the fundamental to its seventh harmonic in the VUV range using a fsEC. The comb has a repetition rate of 75 MHz, and the available power in the seventh harmonic on the target is approximately 200 μW, corresponding to 1 nW per comb mode. The VUV beam has a diameter of 0.2 mm. Through system noise suppression and frequency stabilization, the linewidth of the VUV comb teeth was maintained at less than 300 kHz (FWHM), meeting the requirements for high-resolution nuclear spectroscopy. The measurement was conducted using a ^{229}Th:CaF_2 single crystal with a doping concentration of 5×10^{18} cm^{-3}, dimensions of $1.8 \times 0.7 \times 1.4$ mm^3, and a crystal temperature of 150 K. The researchers irradiated the CaF_2 crystal with the VUV frequency comb and successfully observed the VUV fluorescence emission from the Th nucleus. For the first time, the five lines corresponding to the nuclear quadrupole structure of the ^{229m}Th transition were measured. The central frequencies of four main transition lines were determined with a precision of 2 kHz, and the measured fluorescence lifetime was 641(4) seconds. This result improved the measurement accuracy of the ^{229}Th nuclear transition to the kHz level, advancing experimental nuclear spectroscopy and providing key technical support for the development of high-stability solid-state nuclear clocks.

Building on this work, in 2025, the Ye group further used a VUV frequency comb to investigate the temperature sensitivity of the ^{229}Th nuclear transition in a ^{229}Th:CaF_2 single crystal. They measured the four strongest transitions at three temperatures: 150 K, 229 K, and 293 K. They observed shifts of the unsplit frequency and the electric quadrupole splittings due to decreases in the electron density, electric field gradient, and field-gradient asymmetry at the nucleus as the temperature increases. The $m = \pm 5/2 \rightarrow \pm 3/2$ line (i.e., the ^{229m}Th transition) shifts by only 62(6) kHz over the temperature range, i.e., approximately 0.4 kHz/K, representing a promising candidate for a future solid-state optical clock.[43]

6. Progress in the development of 148 nm VUV frequency combs in China

In China, institutions such as East China Normal University, the Institute of Physics of the Chinese Academy of Sciences (CAS), and the Innovation Academy for Precision Measurement Science and Technology (APM) have also carried out related research on VUV/XUV combs, keeping pace with international developments in this field.

The research team led by Zeng[44] at East China Normal University has conducted studies on coupling schemes for VUV/XUV frequency combs. They proposed an efficient scheme to generate and out-couple extreme ultraviolet frequency combs based on cavity-enhanced noncollinear high-harmonic generation. The harmonics generated around the focus and propagating along the bisectrix of the two crossing fundamental-wave (FW) beams escape from the cavity through the gap between the concave mirrors (along the angle bisector of the FW beam propagation directions), resulting in a direct output coupling of XUV frequency combs. By adjusting the crossing angle of the two fundamental beams at the focal point, as well as the intracavity gas pressure and the fundamental beam power, they simulated the ionization probability and the far-field distribution of the HHG. This approach can significantly enhance both the generation and coupling efficiency of HHG. Subsequent experimental implementations of this method have successfully achieved 60% XUV coupling efficiency.[45] The research team led by Wei[46] at the Institute of Physics, Chinese Academy of Sciences, has also carried out work on the construction of XUV frequency comb systems. In 2012, they conducted systematic simulation studies on the design of a fsEC and experimentally built a six-mirror enhancement cavity. Using broadband femtosecond laser pulses with

a repetition rate of 175 MHz, a pulse duration of 15 fs, and a central wavelength of 790 nm as the driving light source, they achieved an enhancement factor of approximately 10.

The group led by Hua and Liu[47] at APM has carried out systematic work on the development of VUV/XUV frequency combs in China. In 2019, they self-built a kilowatt-level near-infrared fsEC system and successfully generated HHG using xenon gas. The experimental setup is shown in Fig. 6(a). The system employed a Yb-doped fiber laser with a central wavelength of 1038 nm, a repetition rate of 100 MHz, and a pulse duration of 100 fs. Using the fsEC, which utilized an input coupling mirror with $R \approx 99.2\%$ and five additional high-reflectivity mirrors ($R > 99.95\%$), an average intracavity power of 6.08 kW was achieved, corresponding to a power enhancement factor of about 225 and a peak intensity of approximately 4.8×10^{13} W/cm^2. The entire fsEC is placed in a vacuum chamber to avoid the influence of air or dust. The chamber is evacuated with a dry pump and a turbo pump, and a background pressure as low as 10^{-4} Pa can be achieved. To couple the co-propagating HHG light out of the cavity, a 350-μm-thick sapphire plate is placed behind the focus at the Brewster angle for the fundamental laser. The out-coupled HHG is diffracted by a grating and detected by a sodium salicylate plate. Bright fluorescence on the sodium salicylate plate was observed, as shown in the inset of Fig. 6(b), indicating that HHG in the fsEC was generated.

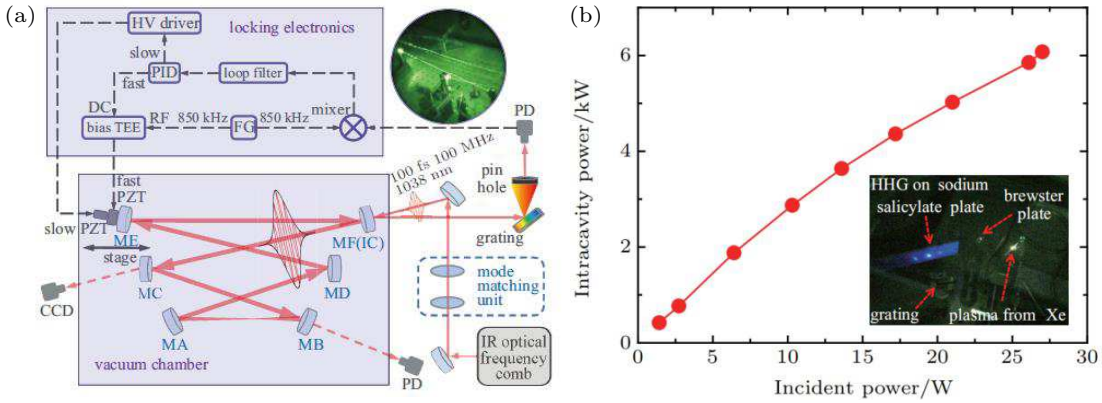


Fig. 6. (a) Schematic view of the six-mirror bowtie fsEC setup. The inset at the upper right shows an IR-viewer photograph of the fsEC under air conditions. The acronyms in the figure are: HV, high voltage; FG, function generator; PZT, piezo transducer; CCD, charge-coupled device; PD, photodetector; IC, input coupler; PID, proportional-integral-derivative circuit; MA(MF), mirror A (mirror F). (b) Intracavity power as a function of incident power. The inset shows a photograph of the focus region of the fsEC.[47]

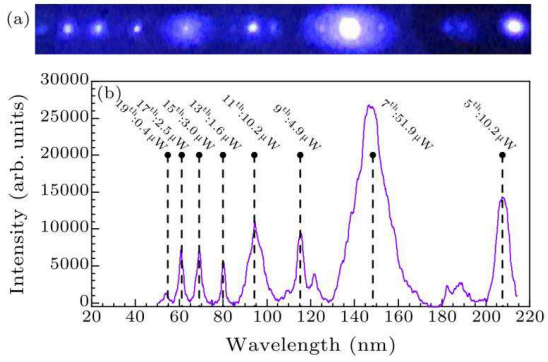


Fig. 7. (a) Image of experimentally observed high-order harmonics fluorescing on a plate coated with sodium salicylate. (b) Spectra of the out-coupled high-harmonic radiation obtained from images of the fluorescent plate. The black dots and the corresponding drop lines indicate the wavelengths of the first-order diffraction.[48]

In 2020, the group at APM further optimized the coupling output scheme and harmonic generation, achieving a frequency comb output in the XUV spectral region.[48] They employed a nanograting as the coupling output scheme, which simultaneously enables extraction and separation of the generated harmonics. The grating parameters were similar to those used in Yost *et al.*[49] With a pump power of 24 W, they achieved an intracavity power of 4.5 kW. As shown in Fig. 7, the experiment successfully obtained harmonic spectra ranging from the 5th to the 19th order. The 7th harmonic (148 nm) reached a power level of 51.9 μW, and in the XUV region, the 11th harmonic (approximately 94 nm) exhibited the highest average power of 10.2 μW.

In 2024, the same group further optimized the pulse duration of the fundamental beam to enhance HHG efficiency and extend the generated XUV spectrum. A Yb-doped fiber laser was used as the driving source, with an output power of 100 W, a pulse duration of 490 fs, and a central wavelength of 1035 nm. Using a photonic crystal fiber and a set of chirped mirrors, the pulse duration was compressed from approximately 490 fs to 56 fs. At an input power of 30 W, an intracavity average power of about 3 kW was achieved, resulting in a peak intensity of 9.3×10^{13} W/cm^2. Based on this, HHG was generated using Xe, Kr, and Ar gases, ultimately achieving XUV radiation with a shortest wavelength of 30 nm (corresponding to the 35th harmonic), as shown in Fig. 8. At 61 nm (the 17th harmonic), the coupled output power reached up to 9.3 μW.[50]

Meanwhile, the APM group measured the linewidth of the home-built 148 nm VUV comb using direct frequency

comb spectroscopy with Xe/NO_2.[51] In an early study, they showed that the beat linewidth between the generated third-order harmonics and the fundamental beam's third harmonic is approximately 3 Hz, indicating that the high-order harmonic process introduces minimal broadening. For direct frequency comb spectroscopy, the 7th harmonic[6,7] was used to excite the single-photon transition of Xe/NO_2 media. The excitation frequency for NO_2 was determined to be 2021.25 THz, with an uncertainty of 0.24 THz (8 cm^{-1}), limited by the tuning range of the repetition frequency. The transition is assigned to $6a_1$ ($v_1' = 0$, $v_2' = 0$) $\rightarrow$ $3p\sigma_u$ ($v_1' = 3$, $v_2' = 8$), where v_1' and v_2' are the symmetrical stretching and bending vibrational frequencies, respectively.[52–54] The upper bound of the VUV comb teeth linewidth was estimated to be less than 28 MHz, as shown in Fig. 9.

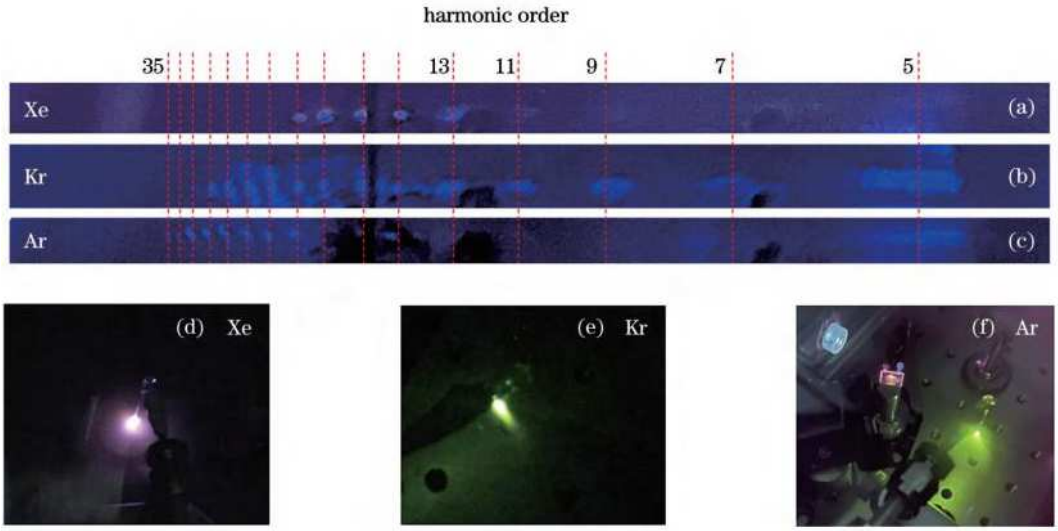


Fig. 8. Fluorescence images obtained using Xe, Kr, and Ar as the gas medium, respectively. (a)–(c) Fluorescence images on a sodium salicylate plate generated by high-order harmonics; (d)–(f) photographs of the plasma and the fluorescence radiation at the gas nozzle.[50]

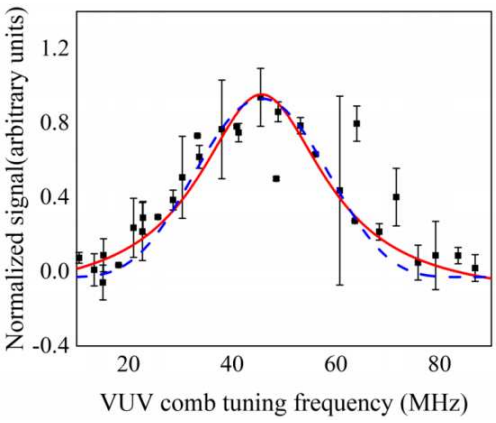


Fig. 9. Average fluorescence signal as a function of the tuning frequency of the VUV comb tooth, obtained from four measurements. The red curve represents a Lorentzian fit to the data, with the best fit corresponding to a linewidth of 29.8 ± 4.5 MHz. The blue dashed line shows a fit using a $\sin^4$ function.[51]

In 2025, the team further increased the power of the 148 nm frequency comb by optimizing the output coupling efficiency, addressing the low out-coupling efficiency of both nano-gratings and Brewster plates (e.g., sapphire and calcium fluoride) at 148 nm. For instance, the diffraction efficiency of the nano-grating at 148 nm was found to be less than 10%, as reported in their work at 2020,[48] and the reflection rate of the sapphire Brewster plate at 148 nm was below 5%, as reported in 2019.[47] To improve the out-coupling efficiency of the 148 nm comb, they customized a batch of CaF_2 Brewster plates with coatings specifically designed for 148 nm. Similar to the previously used sapphire Brewster plate, these CaF_2 plates exhibit high transmittance for 1040 nm laser light at the Brewster angle, but a reflection rate of approximately 80% at 148 nm. By gradually increasing the intracavity average power of the near-infrared frequency comb, they inferred the seventh-order harmonic power from the photodiode current and the reflection rates of the mirrors. The highest measured power of the seventh harmonic was 226.6 μW, as shown in Fig. 10. Considering that the number of comb teeth in the seventh harmonic was on the order of 10^5, the power of each comb tooth was approximately 2.2 nW.

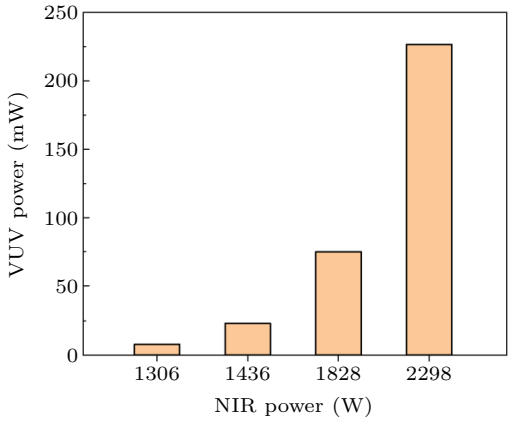


Fig. 10. Measured power of the out-coupled 148 nm VUV frequency comb.

7. Continuous wave 148 nm light source

To ultimately realize a high-precision and stable thorium nuclear clock, developing a CW 148 nm light source is highly desirable to meet key requirements such as narrow linewidth and sufficient power. Currently, there are generally two main approaches to generate a CW 148 nm light source with narrow linewidth: one is the FWM approach using gas media, and the other is the frequency-doubling approach using nonlinear crystals.

In the early stages, Timmermann *et al.*[55] and Nolting *et al.*,[56] as well as other researchers, employed metal vapor media to generate CW VUV radiation through nonlinear processes, with wavelengths demonstrated down to 133 nm. However, the linewidth of these VUV sources was not well characterized. More recently, using a similar technique, the research group led by Ding at Tsinghua University demonstrated 148 nm CW laser generation via FWM in cadmium vapor, achieving a linewidth well below 100 Hz. The scheme of the light source is illustrated in Fig. 11. Two photons (λ_1 and λ_2) at 375 nm, tuned to a two-photon resonance with the 6^1S_0 state, and a third photon (λ_3) at 710 nm are combined and focused into a 50 cm-long cadmium oven held near $T = 550$ °C. The fundamental beams originate from two Ti:sapphire lasers, each locked to a common ultrastable ultralow expansion (ULE) cavity to ensure narrow linewidths. The generated VUV beam is spatially separated from the fundamental beams using a Brewster-angle MgF_2 prism for 148.4 nm. To evaluate phase coherence, the fundamental beams are split and directed into two independent cadmium ovens. The resulting VUV beams are overlapped on a CCD camera with a small crossing angle, producing high-contrast interference fringes that allow direct extraction of the relative optical phase. The source delivers 100 nW of power with a linewidth well below 100 Hz and supports broad wavelength tunability.[57]

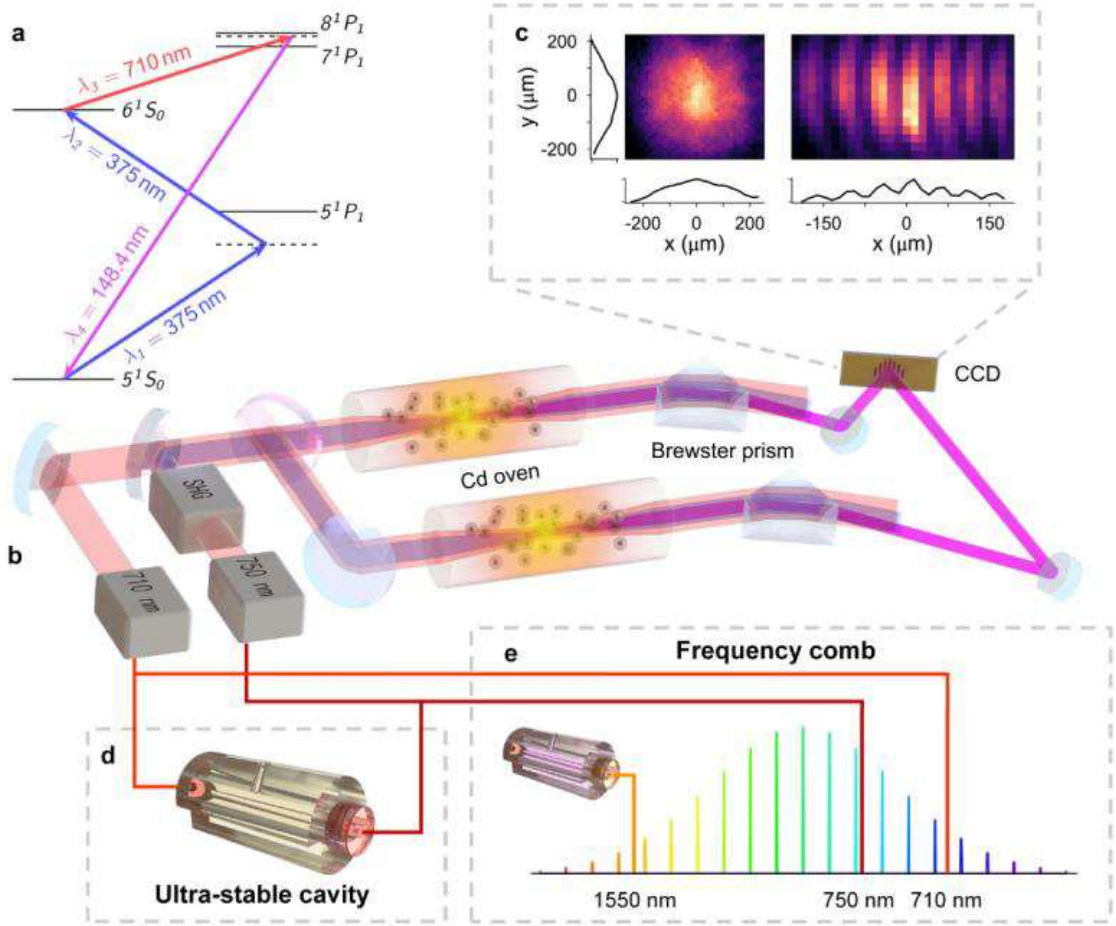


Fig. 11. Generation of a CW VUV laser with narrow linewidth.[57]

In terms of the frequency doubling approach, several crystals, such as $BaMgF_4$ (BMF),[58,59] $KBe_2BO_3F_2$ (KBBF),[60,61] and SrB_4O_7 (SBO)[62–64] are considered as promising candidates owing to their short cut-off wavelengths. However, phase matching for 148 nm light generation with these crystals is extremely challenging, and no CW 148 nm light generation using crystals had been reported for decades.

In 2025, significant breakthroughs were achieved in the

development of CW light sources based on crystals. Peik *et al.* demonstrated a CW laser source at 148.4 nm based on second-harmonic generation (SHG) in randomly quasi-phase matched (RQPM) strontium tetraborate (SBO). They reported three sequential SHG steps starting from a diode laser at 1187 nm, and successfully frequency-doubled CW laser radiation from 296.8 nm to 148.4 nm in a RQPM SBO crystal.

As shown in Fig. 12, the laser radiation is focused into an SBO crystal with dimensions of $0.9 \times 6.4 \times 5.6$ mm^3, placed in a vacuum chamber for the final conversion to 148.4 nm. The temperature-stabilized crystal is mounted on a five-axis translation stage. The SBO used was the same uncoated crystal with an irregular domain structure.[63] Two dichroic mirrors, a VUV grating, and a solar-blind CsI PMT are employed for the detection of the VUV power. The system provided $1.3^{+0.7}_{-0.6}$ nW of VUV power in a single pass for an incident UV laser power of 325 mW.[65]

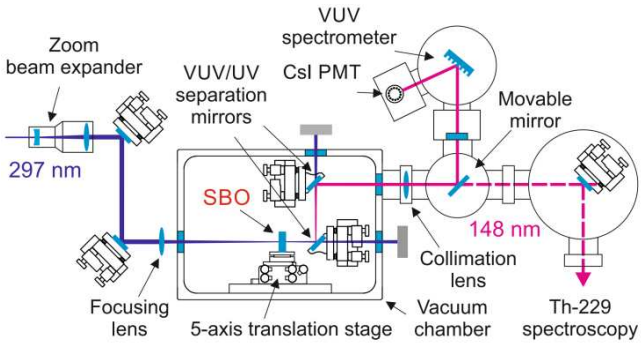


Fig. 12. Experimental setup for SHG at 148.4 nm.[65]

Other than SBO, crystals such as KBBF and BMF are also under development. The KBBF crystal produced by, e.g., the Technical Institute of Physics and Chemistry (TIPC) and the Fujian Institute of Research on the Structure of Matter (FJIRSM), has been mature for VUV light generation for several years.[61–66] At present, efforts focus on optimizing the cutoff wavelength.

In addition, a research group led by Hang[67] at the Shanghai Institute of Optics and Fine Mechanics (SIOM), CAS, has successfully grown high-quality BMF single crystals with considerable size of 30 mm × 60 mm using the Czochralski method. They also investigated the formation mechanism of scattering particles in the $BaMgF_4$ crystal and preliminarily addressed the issue of stray light caused by scattering paths. The group led by Chen[68] at Shanghai Jiao Tong University has conducted studies on the growth of $BaMgF_4$ crystals and successfully produced the largest $BaMgF_4$ single crystal reported to date, with a diameter of approximately 80 mm and a length of about 55 mm. The research group led by Zhu[69] at Nanjing University performed a detailed study on the periodic poling of different crystals, aiming to improve the quasi-phase matching (QPM) of $BaMgF_4$ crystals, making them suitable for generating a 148 nm light source. In 1995, they proposed a method for periodically poling $LiTaO_3$ single crystals at room temperature by applying an external pulsed field. The growth of inverted domains can be controlled by the duration of the pulsed field. A domain structure with period $\Lambda > 8$ pm was fabricated in a 0.3-mm-thick $LiTaO_3$ plate. In 1997, they reported THG achieved through quasi-phase matching technology in a quasi-periodic optical superlattice (QPOS). By designing a Fibonacci sequence structure in $LiTaO_3$ crystals, they directly realized high-efficiency conversion from infrared to green light (with a conversion efficiency of 23%) via SHG and sum-frequency generation (SFG) processes.[70] In 2024, they demonstrated a wafer-scale periodic poling technique on a 4-inch lithium niobate on insulator wafer with high fidelity. The reversal lengths span from 0.5 mm to 10.17 mm, covering an area of ~ 1 cm^2 with periods ranging from 4.38 μm to 5.51 μm. Domain inversion was ultimately implemented across the entire wafer with a 100% success rate and an average 98% high-quality rate.[71]

8. Perspective and outlook

Th-based nuclear optical clocks are widely regarded as promising candidates for next-generation time and frequency standards, with potential precision levels reaching 10^{-20} or beyond. Compared to existing atomic clocks, Th nuclear clocks not only promise to drive a redefinition of the "second", becoming a new global timekeeping benchmark, but also offer exceptional sensitivity to variations in the fine-structure constant. This makes them powerful tools for testing the temporal variation of fundamental constants and exploring physics beyond the Standard Model. Furthermore, the compactness and potential for solid-state integration of nuclear clocks significantly broaden their application prospects in engineering fields such as space-based navigation and geophysical sensing.

As the core technology enabling this nuclear transition, the linewidth, stability, and power of the excitation light source directly determine the excitation efficiency, measurement precision, and ultimately the frequency uncertainty of the nuclear clock. These factors are thus critical for its successful operation. For comparison, the key parameters of the four types of VUV light sources discussed above are listed in Table 1.

Synchrotron radiation sources offer the highest photon energies, broad frequency coverage, and tunable spectral bands. However, in the VUV region, the emitted radiation typically exhibits a relatively broad linewidth, limiting its effectiveness for directly exciting the extremely narrow-bandwidth nuclear transition. Moreover, such facilities are large and immobile. Developing narrow-linewidth synchrotron radiation sources therefore represents a promising direction for future advancement.

Table 1. The realized 148 nm coherent laser sources.

Light sources	Linewidth	Average power	Power spectral density	^{229m}Th excitation
Synchrotron radiation[25]	46 THz	1.3 mW	0.03 fW/Hz	unsuccessful
Pulsed FWM[21,30]	4–10 GHz	450–1200 μW	0.1–0.3 pW/Hz	successful
Pulsed FWM[7,31,32]	10–15 GHz	30–240 μW	2–24 fW/Hz	successful
Frequency comb[2,43]	300 kHz	∼ 1 nW	∼ 3.3 fW/Hz	successful
CW FWM[57]	100 Hz	100 nW	1 nW/Hz	
CW SHG[65]	∼ 100 kHz	1.3 nW	∼ 10 fW/Hz	

The FWM method with pulsed lasers features relatively simple experimental setups and significantly lower cost compared to synchrotron radiation sources, making it accessible in standard laboratory environments. It can generate higher VUV pulse energies and offers a broad range of frequency tunability. However, the typical linewidth of FWM-generated pulsed VUV light remains at the GHz level, limiting spectral resolution. In the future, the development of narrow-linewidth FWM pulsed sources will be a valuable and promising research direction.

The greatest advantage of VUV optical frequency combs lies in their frequency tunability and high spectral resolution. Each comb tooth corresponds to a stable and precisely known absolute frequency, determined by $f_n = n \cdot f_r + f_0$, both of which can be accurately controlled. This makes VUV combs ideally suited for probing ultra-narrow nuclear transitions, such as those in ^{229m}Th. By locking the VUV optical frequency comb to an atomic clock, a measurement uncertainty at the kHz level can be achieved. Fine tuning of the repetition rate allows precise scanning across the entire spectral region. The linewidth of each comb tooth is significantly narrower than the natural linewidth of the ^{229}Th nuclear transition in a crystal, enabling high-resolution spectral discrimination. However, the power of each individual comb tooth remains limited, and compared to other light sources, the operational stability of VUV combs is still constrained, making continuous long-term operation (on the scale of days) challenging at present. Moreover, unused comb teeth contribute noise to the experiment, which must be well suppressed.

CW light sources offer several advantages, including narrow linewidth, concentrated power, stable frequency, and continuous temporal structure. At present, two approaches have been demonstrated to realize a CW 148 nm source: one based on SHG in SBO crystals and the other on four-wave mixing in cadmium vapor. These light sources will greatly promote the development of the Th nuclear clock. Nevertheless, further efforts are still required to improve their performance. For example, the main limitation for SBO lies in achieving reproducibility and higher efficiency in the RQPM process. Additionally, BMF and KBBF crystals are considered promising candidates, and further work is required to develop phase-matching techniques for $BaMgF_4$, while optimizing absorption near 148 nm is necessary for KBBF.

Acknowledgments

This project is supported by the Strategic Priority Research Program of the Chinese Academy of Sciences (Grant No. XDB0920000), the National Natural Science Foundation of China (Grant Nos. 12121004 and U21A20435), the Chinese Academy of Sciences Project for Young Scientists in Basic Research (Grant No. YSBR-055), and the Science and Technology Department of Hubei Province (Grant No. 2025AFA004).

References

[1] Peik E, Schumm T, Safronova M S, Palffy A, Weitenberg J and Thirolf P G 2021 *Quantum Sci. Technol.* **6** 034002
[2] Zhang C, Ooi T, Higgins J S, *et al.* 2024 *Nature* **633** 63
[3] Yamaguchi A, Shigekawa Y, Haba H, Kikunaga H, Shirasaki K, Wada M and Katori H 2024 *Nature* **629** 62
[4] Kraemer S, Moens J, Athanasakis-Kaklamanakis M, Bara S, Beeks K, Chhetri P, Chrysalidis K, Claessens A, Cocolios T E, Correia J G M, Witte H D, Ferrer R, Geldhof S, Heinke R, Hosseini N, Huyse M, Köster U, Kudryavtsev Y, Laatiaoui M, Lica R, MagchielsG, Manea V, Merckling C, Pereira L M C, Raeder S, Schumm T, Sels S, Thirolf P G, Tunhuma S M, Van Den Bergh P, Van Duppen P, Vantomme A, Verlinde M, Villarreal R and Wahl U 2023 *Nature* **617** 706
[5] Hiraki T, Okai K, Bartokos M, Beeks K, Fujimoto H, Fukunaga Y, Haba H, Kasamatsu Y, Kitao S, Leitner A, Masuda T, Guan M, Nagasawa N, Ogake R, Pimon M, Pressler M, Sasao N, Schaden F, Schumm T, Seto M, Shigekawa Y, Shimizu K, Sikorsky T, Tamasaku K, Takatori S, Watanabe T, Yamaguchi A, Yoda Y, Yoshimi A and Yoshimura K 2024 *Nat. Commun* **15** 5536
[6] Tiedau J, Okhapkin M V, Zhang K, Thielking J, Zitzer G, Peik E, Schaden F, Pronebner T, Morawetz I, De Col L T, Schneider F, Leitner A, Pressler M, Kazakov G A, Beeks K, Sikorsky T and Schumm T 2024 *Phys. Rev. Lett.* **132** 182501
[7] Elwell R, Schneider C, Jeet J, Terhune J E S, Morgan H W T, Alexandrova A N, Tran Tan H B, Derevianko A and Hudson E R 2024 *Phys. Rev. Lett.* **133** 013201
[8] Campbell C J, Radnaev A G, Kuzmich A, Dzuba V A, Flambaum V V and Derevianko A 2012 *Phys. Rev. Lett.* **108** 120802
[9] Fadeev P, Berengut J C and Flambaum V V 2020 *Phys. Rev. A* **102** 052833
[10] Dzuba V A, Flambaum V V and Webb J K 1999 *Phys. Rev. Lett.* **82** 888
[11] Dzuba V A, Flambaum V V and Webb J K 1999 *Phys. Rev. A* **59** 230
[12] Huntemann N, Lipphardt B, Tamm C, Gerginov V, Weyers S and Peik E 2014 *Phys. Rev. Lett.* **113** 210802
[13] Flambaum V V and DzubaV A 2009 *Can. J. Phys.* **87** 25
[14] Dzuba V A, Flambaum V V and Schiller S 2018 *Phys. Rev. A* **98** 022501
[15] Safronova M S 2019 *Ann. Phys. (Berlin)* **531** 1800364
[16] Tong X, Hua L, Hua X and Liu X 2025 *Natl. Sci. Rev.* nwaf083
[17] Kroger L A and Reich C W 1976 *Nucl. Phys. A* **259** 29
[18] Beck B R, Becker J A, Beiersdorfer P, Brown G V, Moody K J, Wilhelmy J B, Porter F S, Kilbourne C A and Kelley R L 2007 *Phys. Rev. Lett.* **98** 142501

[19] Yamaguchi A, Muramatsu H, Hayashi T, *et al.* 2019 *Phys. Rev. Lett.* **123** 222501

[20] Sikorsky T, Geist J, Hengstler D, *et al.* 2020 *Phys. Rev. Lett.* **125** 142503

[21] Tiedau J, Okhapkin M V, Zhang K, *et al.* 2024 *Phys. Rev. Lett.* **132** 182501

[22] Margaritondo G 2022 *J. Vac. Sci. Technol. A* **40** 033204

[23] Schwinger J 1949 *Phys. Rev.* **75** 1912

[24] SPRING - 8 SRS 2005 *A Brief Introduction of Spring - 8 SRS* (Hyogo: Spring-8) pp. 2–6

[25] Jeet J, Schneider C, Sullivan S T, *et al.* 2015 *Phys. Rev. Lett.* **114** 253001

[26] Stellmer S, Kazakov G, Schreitl M, Kaser H, Kolbe M and Schumm T 2018 *Phys. Rev. A* **97** 062506

[27] Masuda T, Yoshimi A, Fujieda A, *et al.* 2019 *Nature* **573** 238

[28] Tao Y, Huang Y, Gao Z, Zhuang H, Zhou A, Tan Y, Li D and Sun S 2009 *Synchrotron Rad.* **16** 857

[29] Sun Z P, Liu Z H, Liu Z T, Liu W L, Zhang F Y, Shen D W, Ye M and Qiao S 2020 *Synchrotron Rad.* **27** 1388

[30] Thielking J, Zhang K, Tiedau J, Zander J, Zitzer G, Okhapkin M V and Peik E 2023 *New J. Phys.* **25** 083026

[31] Zhang C, von der Wense L, Doyle J F, *et al.* 2024 *Nature* **636** 603

[32] Elwell R, Terhune J E S, Schneider C, *et al.* 2025 *Nature* **648** 300

[33] Wang J 2018 *Apparatus and Applications of Vacuum Ultraviolet Laser Desorption/ IonizationMass Spectrometry Imaging* (Ph.D. Dissertation) (Beijing: Tsinghua University) (in Chinese)

[34] Zang J 2021 *Generation of a Frequency Comb in the Extreme Ultraviolet* (Ph.D. Dissertation) (Beijing: University of Chinese Academy of Sciences) (in Chinese)

[35] Corkum P B 1993 *Phys. Rev. Lett.* **71** 1994

[36] Jones R J, Moll K D, Thorpe M J and Ye J 2005 *Phys. Rev. Lett.* **94** 193201

[37] Gohle C, Udem T, Herrmann M, Rauschenberger J, Holzwarth R, Schuessler H A, Krausz F and Hänsch T W 2005 *Nature* **436** 234

[38] Cingöz A, Yost D C, Allison T K, Ruehl A, Fermann M E, Hartl I and Ye J 2012 *Nature* **482** 68

[39] Pupeza I, Holzberger S, Eidam T, *et al.* 2013 *Nat. Photonics* **7** 608

[40] Benko C, Allison T K, Cingöz A, Hua L, Labaye F, Yost D C and J Ye 2014 *Nat. Photonics* **8** 530

[41] Porat G, Heyl C M, Schoun S B, Benko C, Dörre N, Corwin K L and Ye J 2018 *Nat. Photonics* **12** 387

[42] Aeppli A, Kim K, Warfield W, Safronova M S and Ye J 2024 *Phys. Rev. Lett.* **133** 023401

[43] Higgins J S, Ooi T, Doyle J F, Zhang C, Ye J, Beeks K, Sikorsky T and Schumm T 2025 *Phys. Rev. Lett.* **134** 113801

[44] Wu J and Zeng H 2007 *Opt. Lett.* **32** 3315

[45] Zhang C, Schoun S B, Heyl C M, Porat G, Gaarde M B and Ye J 2020 *Phys. Rev. Lett.* **125** 093902

[46] Han H N, Zhang J W, Zhang Q, Zhang L and Wei Z Y 2012 *Acta Phys. Sin.* **61** 164206 (in Chinese)

[47] Zhang J, Hua L Q, Yu S G, Chen Z and Liu X J 2019 *Chin. Phys. B* **28** 044206

[48] Zhang J, Hua L Q, Chen Z, Zhu M F, Gong C and Liu X J 2020 *Chin. Phys. Lett.* **37** 124203

[49] Yost D C, Schibli T R and Ye J 2008 *Opt. Lett.* **33** 1099

[50] Zhang H Z, Zhu M F, Xiao Z R, Hua L Q, Xu S P, Liu Y N and Liu X J 2024 *Acta Opt. Sin.* **44** 299 (in Chinese)

[51] Zhu M F, Xiao Z R, Zhang H Z, Hua L Q, Liu Y N, Zuo Z, Xu S P and Liu X J 2024 *Opt. Lett.* **49** 3757

[52] Nakayama T, Kitamura M Y and Watanabe K 1959 *J. Chem. Phys.* **30** 1180

[53] Morioka Y, Masuko H, Nakamura M, Sasanuma M and Ishiguro E 1978 *Can. J. Phys.* **56** 962

[54] Ritchie R K and Walsh A D 1962 *Proc. R. Soc. Lond. A* **267** 395

[55] Timmermann A and Wallenstein R 1983 *Opt. Lett.* **8** 517

[56] Nolting J, Kunze H, Schütz I and Wallenstein R 1990 *Appl. Phys. B* **50** 331

[57] Xiao Q, Penyazkov G, Li X, *et al.* 2025 arXiv:2507.19449v1 [physics.atom-ph]

[58] Buchter S C, Fan T Y, Liberman V, Zayhowski J J, Rothschild M, Mason E J, Cassanho A, Jenssen H P and Burnett J H 2001 *Opt. Lett.* **26** 1693

[59] Villora E G, Shimamura K, Sumiya K and Ishibashi H 2009 *Opt. Express* **17** 12362

[60] Kang L and Lin Z 2022 *Light Sci. Appl.* **11** 201

[61] Nakazato T, Ito I, Kobayashi Y, Wang X, Chen C and Watanabe S 2016 *Opt. Express* **24** 17149

[62] Baudrier-Raybaut M, Haidar R, Kupecek P, Lemasson P and Rosencher E 2004 *Nature* **432** 374

[63] Trabs P, Noack F, Aleksandrovsky A S, Zaitsev A I and Petrov V 2016 *Opt. Lett.* **41** 618

[64] Philipp H R and Taft E A 1956 *J. Phys. Chem. Solids* **1** 159

[65] Lal V, Okhapkin M V, Tiedau J, Irwin N, Petrov V and Peik E 2025 *Optica* **12** 1971

[66] Nomura Y, Ito Y, Ozawa A, Wang X, Chen C, Shin S, Watanabe S and Kobayashi Y 2011 *Opt. Lett.* **36** 1758

[67] Zhao C, Zhang L, Hang Y, *et al.* 2011 *J. Cryst. Growth* **316** 158

[68] Wang Z 2018 *Research on Growth and Nonlinear Optical Properties of* $Bamgf_4$ *Crystal and Microcrystal* (Ph.D. Dissertation) (Shanghai: Shanghai Jiao Tong University) (in Chinese)

[69] Zhu S, Zhu Y, Zhang Z, *et al.* 1995 *J. Appl. Phys.* **77** 5481

[70] Zhu S, Zhu Y and Ming N 1997 *Science* **278** 843

[71] Chen M, Wang C, Tian X H, *et al.* 2024 *Materials* **17** 1720